DEVELOPMENT OF A SCROLL COMPRESSOR MODEL FOR PROPANE

Paul Byrne, Redouane Ghoubali, Jacques Miriel

DEVELOPMENT OF A SCROLL COMPRESSOR MODEL FOR PROPANE

Paul Byrne[(a)], Redouane Ghoubali[(a)] and Jacques Miriel[(a)]

[(a)] Université Européenne de Bretagne, Equipe MTRhéo, Laboratoire LGCGM,
INSA de Rennes et Université de Rennes1
IUT Génie Civil, 3 rue du Clos Courtel, BP 90422, 35704 Rennes Cedex 7, paul.byrne@univ-rennes1.fr

ABSTRACT

Hydrocarbons are today considered as promising alternative substances because of their low environmental impact and their easy implementation in heat pumps. The heat pumping technology is similar to that of HFCs. However, some precautions have to be taken to thwart their flammability. European regulations impose stringent certifications (ATEX, Atmosphères Explosives) on components and an installation outside the buildings for devices having the refrigerant charge of small heat pumps for space heating.

In the frame of a research project on heat pumps for simultaneous heating and cooling (HPS), an R407C prototype of air-source HPS was built and tested. A second prototype is today being designed for propane. A simple and thermodynamically realistic model was developed using EES software. It is an adaptation of an R407C model validated with experimental data. The development of this scroll compressor model working with R407C and its adaptation to thermodynamic properties of propane is presented in this article. A comparison is finally carried out between R407C and R290 scroll compressor models.

1. INTRODUCTION

The study presented in this article is part of a project on heat pumps for simultaneous heating and cooling (HPS) (Byrne et al. 2009). A first prototype providing 15 kW heating capacity was built and tested (Byrne et al. 2011a). It can produce hot and cold water in two different water tanks at the same time (simultaneous mode), only hot water (heating mode) or only cold water (cooling mode). The main characteristic of the HPS is to operate using an alternation of modes. During a heating mode in winter, the HPS produces heat and also stores some energy recovered by subcooling of the refrigerant in the cold water tank (not used for cooling during winter). The water tank temperature then rises and the simultaneous mode is launched. During the operation under the simultaneous mode, the heat pump performance is increased because of a higher evaporating temperature using a temperature-controlled water source than using ambient air. Moreover, during that mode, the air evaporator is unused and free for defrosting. A previous study has demonstrated the mechanism of a two-phase thermosiphon defrosting technique (Byrne et al. 2011b). The thermosiphon is created between the water evaporator, being the evaporator of the thermosiphon, and the air evaporator, being the condenser of the thermosiphon. This under-development technique carries out defrosting without stopping the heat production.

Hydrocarbons are positioned as natural alternative refrigerants to halogenated substances. Their environmental impact is very low in terms of global warming. For instance, the GWP of propane (R290) over a 100-year horizon is equal to 3. Performance of hydrocarbons is comparable to that of the fluorinated fluids in the same range of pressures. They are already widely used in household applications like domestic refrigerators. These features imply that hydrocarbons are also envisaged as drop-in substitutes to HFCs in heat pumps using the same technology. A nuance can be formulated concerning precautions to avoid contact between the refrigerant and components likely to generate sparks such as rotating pieces of the compressor or solenoid valves. However, scroll compressors are usually of a higher power range than the compressors for domestic refrigerators. Nevertheless, a study presented by Adamson (2008) proves that ATEX-certified scroll compressors for hazardous areas exist. The ATEX certification is necessary to use R290 as a refrigerant.

A second HPS prototype, simplified and industry-oriented, is currently under design. The chosen refrigerant is R290. A simulation study has to be executed to evaluate the operating parameters of the HPS using this

new fluid. The complete model describing the components in detail was presented in a paper presented at the 2008 Gustav Lorentzen Conference (Byrne et al. 2008). A special focus is made here on the compressor model that has been improved since that previous publication in the sense that it is now thermodynamically realistic.

Several studies were already carried out on more or less detailed compressor modelling. Chen et al. (2002a and 2002b) worked on a mathematical modelling of scroll compressors. A geometry study was conducted for the suction, compression and discharge chambers of the compressor. It combines the models of refrigerant flows in the suction and discharge processes, radial and flank leakage and heat transfers between the refrigerant and the scroll wraps. Blunier et al. (2009) developed a similar geometry description of the scroll compressor model. Tseng and Chang (2006) and Sun et al. (2010) also propose a design optimization of the scroll compressor using mathematical models.

Duprez et al. presented two papers (2007 and 2010) on a modelling technique for reciprocating and scroll compressors. This semi-empirical technique is simple and thermodynamically realistic. Accurate results are also obtained, having average deviations less than 3% for scroll compressors. Kinab et al. (2010) proposed a global heat pump model for seasonal performance optimization. It also uses a semi-empirical model for the compressor and leads to results in pretty good agreement with those of a test bench. Cuevas and Lebrun (2009), Cuevas et al. (2010), Winandy et al. (2002a), Winandy and Lebrun (2002b) worked on a simplified scroll compressor model based on the main processes affecting the refrigerant during compression. It uses a fictitious wall to model heat exchanges within the compressor. It is able to compute the following variables: mass flow rate, power input, discharge temperature, suction heating-up, discharge cooling-down and ambient losses.

The objective of this paper is to present the development of a simplified compressor model for future performance evaluation of a heat pump for simultaneous heating and cooling working with R290. It is an adaptation of the numerical model developed by Winandy et al. (2002a) using special assumptions, some of which are inspired by Duprez et al. (2007 and 2010). The model was first constructed for a scroll R407C compressor and validated using experimental results and then adapted to refrigerant R290. A comparison is finally carried out to evaluate the mass flow rate and input power discrepancies and discharge temperature differences between R407C and R290 models.

2. MODEL DEVELOPMENT

This section describes the modelling procedure we used to develop our scroll compressor model and the validation steps by comparison with experimental data obtained on an Emerson Copeland ZB38KCE scroll compressor. It is based on the model of Winandy et al. (2002a) in which the refrigerant state is decomposed. The simulation software is EES (Klein and Alvarado, 2000). The model calculates the refrigerant mass flow rate, the input power and the discharge temperature using the suction temperature and high and low pressures as input variables and internal heat exchange coefficients as parameters.

2.1 General equations

Transformations applied to the refrigerant through the compressor can be defined following figure 1. Three steps are involved: suction heating-up (from su to su1), polytropic compression (from su1 to ex1) and discharge cooling down (from ex1 to ex). $\dot{W}_{loss}$ corresponds to electromechanical losses and $\dot{W}_{in}$ to the internal compression power delivered to the refrigerant. The refrigerant mass flow rate is given by equation 1 where V_s in m^3/s is the constant swept volume provided by the manufacturer and v_{su1} is the specific volume at the end of the suction heating-up process.

$$\dot{m} = \frac{V_s}{v_{su1}} \tag{1}$$

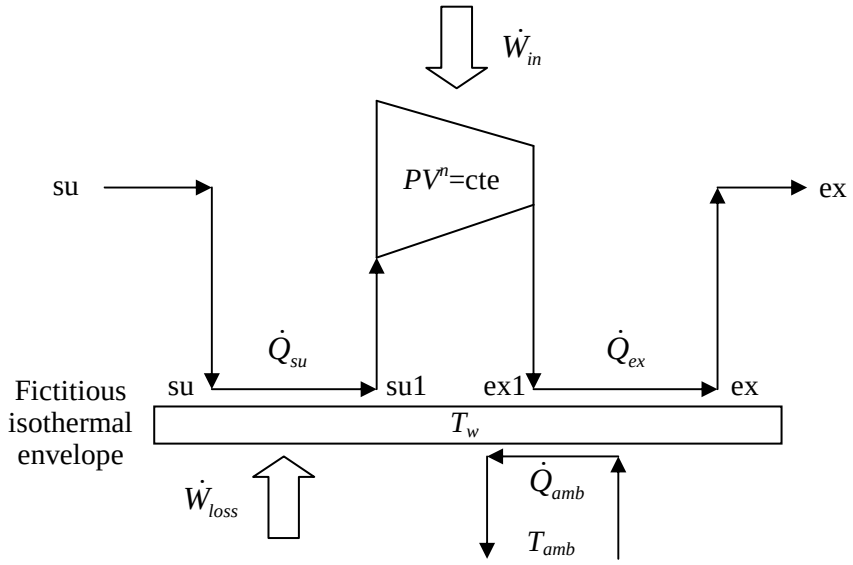

Figure 1. Refrigerant transformations through the compressor model

The fictitious wall is in steady state at a constant temperature, like in the publication of Duprez et al. (2007), at a mean value between temperatures at points ex and su1 following equation 2.

$$T_w = \frac{T_{ex} + T_{su1}}{2} \tag{2}$$

Heat transfers with the fictitious wall are supposed to be balanced and equation 3 can be stated.

$$\dot{W}_{loss} + \dot{Q}_{ex} - \dot{Q}_{su} - \dot{Q}_{amb} = 0 \tag{3}$$

Heat exchange at suction heating-up can be modelled using the DTLM method (Equation 4)

$$\dot{Q}_{su} = UA_{su} \cdot \left(\frac{T_{su1} - T_{su}}{\ln \frac{T_w - T_{su}}{T_w - T_{su1}}} \right) \tag{4}$$

This thermal capacity is also defined by equation 5.

$$\dot{Q}_{su} = \dot{m} \cdot \left(h_{su1} - h_{su} \right) \tag{5}$$

The same set of equations is used for discharge cooling down (Equations 6 and 7).

$$\dot{Q}_{ex} = UA_{ex} \cdot \left(\frac{T_{ex1} - T_{ex}}{\ln \frac{T_{ex} - T_w}{T_{ex1} - T_w}} \right) \tag{6}$$

$$\dot{Q}_{ex} = \dot{m} \cdot \left(h_{ex1} - h_{ex} \right) \tag{7}$$

Heat transfer towards the environment can be calculated using equation 8, where T_{amb} is assumed to be constant and equal to 20 °C.

$$\dot{Q}_{amb} = UA_{amb} \cdot (T_w - T_{amb}) \quad (8)$$

During the internal compression, the refrigerant state evolution follows equation 9 using a constant polytropic exponent *n*.

$$\dot{W}_{in} = \frac{n}{n-1} LP \cdot \dot{m} \cdot v_{su1} \cdot \left(\left(\frac{HP}{LP} \right)^{\frac{n-1}{n}} - 1 \right) \quad (9)$$

Finally, the compressor shaft power is given by equation 10.

$$\dot{W} = \dot{W}_{in} + \dot{W}_{loss} \quad (10)$$

The other hypotheses made in this model are the following.

- Pressure drops are neglected inside the compressor crankcase.
- Superheat is constant and equal to 5 K.
- Heat transfer coefficients are constant.
- Polytropic exponent is constant and equal to 1.4.

2.2 Determination of parameters

In a first simulation, UA_{su}, UA_{amb} and UA_{ex} are unknown. These coefficients are assumed to be constant parameters of the model. Their determination for R407C is carried out using values of the mass flow rate, the shaft power and the discharge temperature measured on our R407C prototype for nominal operating conditions. Table 1 shows the nominal values of main variables and parameters for an evaporating temperature of 0 °C and a condensing temperature of 50 °C at dew points.

Table 1. Main variables and parameters at nominal conditions for R407C model

T_{ev} (°C)	T_{cd} (°C)	T_w (°C)	T_{su} (°C)	T_{su1} (°C)	T_{ex1} (°C)	T_{ex} (°C)	$\dot{m}$ (kg/s)	$\dot{W}$ (W)	UA_{su} (W/K)	UA_{amb} (W/K)	UA_{ex} (W/K)
0	50	46.06	5	12.57	83.29	79.56	0.07217	4204	12.38	26.73	8.094

2.3 Model validation

The model validation is carried out using experimental results obtained on the R407C HPS prototype. The ranges of evaporating and condensing temperatures are respectively -7 °C to +10 °C and 40 °C to 55 °C. They correspond to the temperatures used in the applications of the HPS, which are domestic hot water preheating and space heating and cooling in oceanic climate regions. The following figures show satisfactory accordance between experimental and modelled values.

Figure 2 shows a correct agreement between experimental and modelled mass flow rates. The maximum discrepancy is less than 9.2%.

Figure 3 shows the comparison between experimental and modelled shaft power at the compressor. Lower values of input power are underestimated by the model down to -14.7%. This discrepancy can come from an underestimation of the constant part of electromechanical losses described by Winandy et al. (2002) for the lower values of compression ratio. The maximal discrepancy is 6.2%. In addition, since scroll compressors have fixed built-in volume, the trend shown in figure 3 can be explained by the fact that the isentropic efficiency of the compressor effectively changes in the range of the considered pressure ratios (between 2.25 and 5.52). However we considered a fixed polytropic exponent to calculate the compression work. In a future version, correcting this assumption will participate to the improvement of the model.

Figure 4 shows a correct agreement between experimental and modelled discharge temperature. Temperature differences are included in an interval from -5.2 K to +4.2 K. The discharge temperature will

be used in the global heat pump model as an input variable for the condenser model. Therefore achieving satisfactory accuracy on this output variable is also very important.

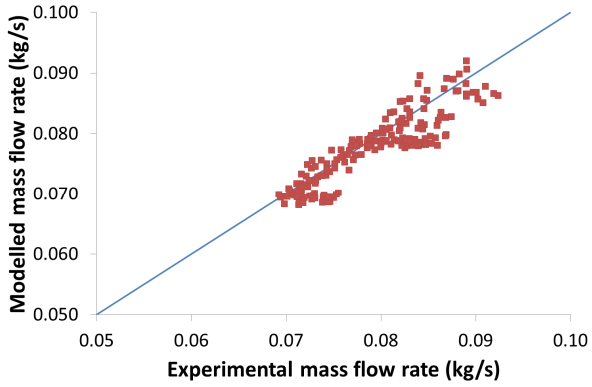

Figure 2. Comparison between experimental and modelled mass flow rate

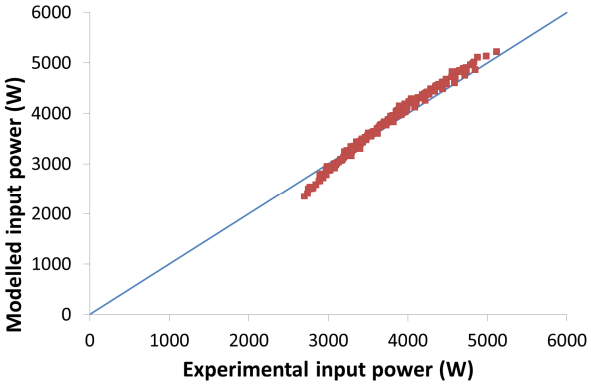

Figure 3. Comparison between experimental and modelled input power

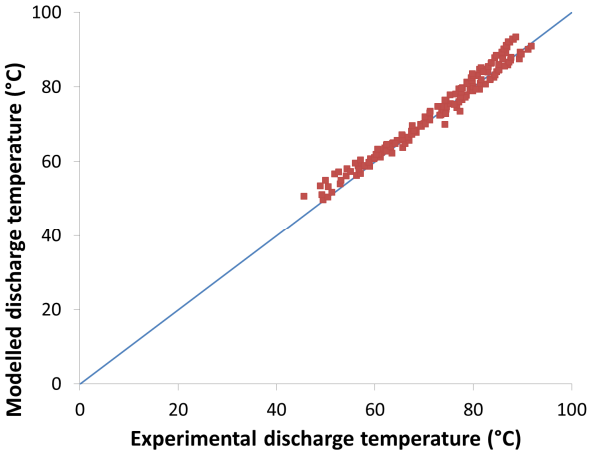

Figure 4. Comparison between experimental and modelled discharge temperature

3. MODEL ADAPTATION FOR R290

The new model corresponds to the same compressor adapted to thermodynamic properties of propane. In this section, the model adaptation is presented and a comparison between R407C and R290 models is led.

3.1 Assumptions for model adaptation to R290

The adaptation of the model consists in recalculating the heat transfer coefficients at suction UA_{su} and discharge UA_{ex} for nominal conditions of evaporation at 0 °C and condensation of 50 °C. The U value is assumed to be calculated using the Nusselt number following equation 11. Nusselt number Nu and conductivity λ depend on the fluid. Nusselt number is given by Dittus-Boelter correlation (equation 12), where parameter m is equal to 0.4 for the suction heating process and 0.3 for the discharge cooling process. Reynolds number Re depends on the viscosity ν of the fluid (equation 13). In equations 11 to 13, characteristic length L, velocity V (linked to swept volume V_s) and hydraulic diameter D are geometric parameters of the scroll compressor and are the same for R290 as for R407C. The adaptation to propane properties results in equation 14 for UA_{su} and UA_{ex} values. UA_{amb} is independent on the refrigerant and has the same value as for R407C.

$$U = \frac{\mathrm{Nu} \cdot \lambda}{L} \tag{11}$$

$$\mathrm{Nu} = 0.023 \cdot \mathrm{Re}^{0.8} \cdot \mathrm{Pr}^{m} \tag{12}$$

$$\mathrm{Re} = \frac{V \cdot D}{\nu} \tag{13}$$

$$UA_{R290} = UA_{R407C} \cdot \left(\frac{\nu_{R407C}}{\nu_{R290}} \right)^{0.8} \cdot \left(\frac{\mathrm{Pr}_{R290}}{\mathrm{Pr}_{R407C}} \right)^{m} \cdot \left(\frac{\lambda_{R290}}{\lambda_{R407C}} \right) \tag{14}$$

A second adaptation is carried out on the polytropic exponent n_{R290} used in equation 9. It is recalculated depending on the ratio of isentropic exponents γ_{R290} and γ_{R407C} (equation 15).

$$n_{R290} = n_{R407C} \cdot \left(\frac{\gamma_{R290}}{\gamma_{R407C}} \right) \tag{15}$$

The results of the adaptation to propane are reported in table 2.

Table 2. Values of thermodynamic properties at nominal conditions for R407C and R290 models

Refrigerant	$\mathbf{Pr}_{su}$ **(-)**	λ_{su} **(W.m^{-1}.K^{-1})**	ν_{su} **(m^2.s^{-1})**	$\mathbf{Pr}_{ex}$ **(-)**	λ_{ex} **(W.m^{-1}.K^{-1})**	ν_{ex} **(m^2.s^{-1})**	γ **(-)**	n **(-)**
R407C	0.7763	0.01366	$7.263 \cdot 10^{-7}$	0.8832	0.01844	$1.955 \cdot 10^{-7}$	1.187	1.4
R290	0.8240	0.01818	$9.006 \cdot 10^{-7}$	1.029	0.02377	$2.705 \cdot 10^{-7}$	1.195	1.409

3.2 Comparison of R407C and R290 models

A comparison of mass flow rates, input powers and discharge temperatures is finally carried out between R407C and R290 in the same range of evaporating temperatures (-7 °C to +10 °C) and condensing temperatures (40 °C to 55 °C).

Figure 5 shows R290 mass flow rate compared to the one of R407C using the same compressor. The ratio between R407C and R290 values is nearly constant. The R290 mass flow rate is 45.4% lower than the R407C one. This discrepancy acts in an unfavourable manner for R290 scroll compressor because the heating or cooling capacities are proportional to the mass flow rate. Nevertheless the ratio of latent heat recoverable by condensation at 50 °C of R407C over the one of R290 is in the same proportion than the inverse ratio of mass flow rates. So the heating capacity recoverable by implementing R290 instead of R407C should be somewhat equivalent.

Figure 6 presents the comparison between input powers. The average decrease is 12.4%. This discrepancy acts in a favourable manner concerning the heat pump COP.

Figure 7 shows the difference between discharge temperatures using R407C and R290 models. The difference varies from 6.4 K to 12.0 K. It is a good result in terms of longevity of the compressor and prevention of oil deterioration. Besides, the desuperheating process will be decreased compared to an operation with the same discharge temperatures as the ones of R407C. However, the specific heat of R290 is twice the one of R407C in vapour phase at these pressures. So the heating capacity recoverable during the desuperheating process using R290 will be equivalent or even higher than that of R407C.

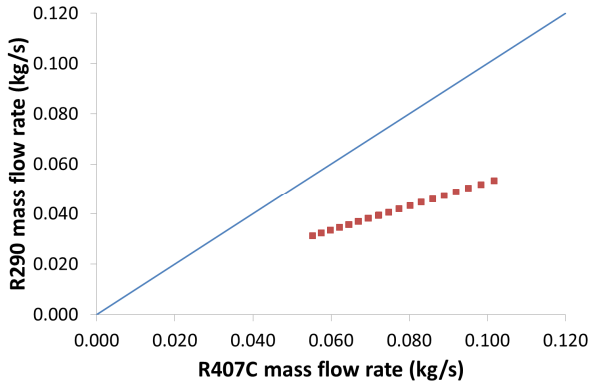

Figure 5. Comparison between R407C and R290 modelled mass flow rate

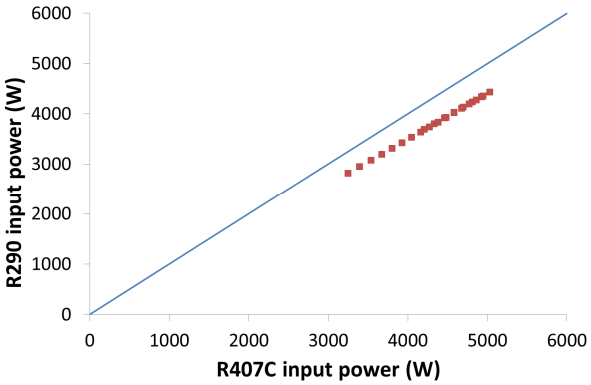

Figure 6. Comparison between R407C and R290 modelled input power

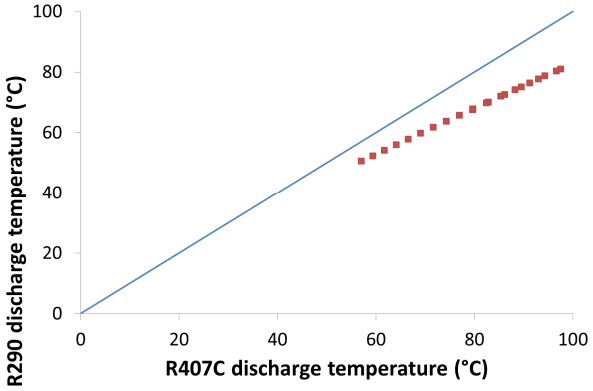

Figure 7. Comparison between R407C and R290 modelled discharge temperature

4. CONCLUSIONS

This study is part of a research project on heat pumps for simultaneous heating and cooling. A simple and thermodynamically realistic R407C scroll compressor model was developed and adapted to refrigerant R290, a promising fluid with regard to the evolution of international regulations. The Winandy et al. (2002a) model was used with some assumptions made by Duprez et al. (2007 and 2010). A difference was brought in our model concerning the internal power calculation by the use of a polytropic evolution during compression. The model considers constant heat transfer coefficients at suction heating-up, discharge cooling down and transfer to the ambient. These assumptions are linked to the discrepancies between experimental and modelled results. During the model development, we noticed that there is a non-negligible variation of *UA* values depending on refrigerant and wall temperatures, thus on Nusselt numbers and convection heat transfer coefficients. Further development of the scroll compressor model will concern the redefinition of these parameters. Another improvement path relies in the redefinition of the polytropic exponent, assumed constant in this study but actually dependent on the pressure ratio. The comparison study between R407C and R290 models concludes a possible performance improvement by implementing R290 in the R407C scroll compressor. The next step of this work will be the comparison of the results of our R290 model with the ones of an experimental study carried out on an R290 HPS prototype. This R290 model will then be implemented in a heat pump for simultaneous heating and cooling model for seasonal performance evaluation.

NOMENCLATURE

A	heat exchanger surface area (m^2)	D	hydraulic diameter (m)
γ	isentropic exponent (-)	h	specific enthalpy ($J \cdot kg^{-1} \cdot K^{-1}$)
HP	high pressure (Pa)	L	characteristic length (m)
LP	low pressure (Pa)	λ	conductivity ($W \cdot m^{-1} \cdot K^{-1}$)

$\dot{m}$	mass flow rate ($kg \cdot s^{-1}$)	n	polytropic exponent (-)
Nu	Nusselt number (-)	ν	viscosity ($m^2 \cdot s^{-1}$)
Pr	Prandtl number (-)	$\dot{Q}$	thermal capacity (W)
Re	Reynolds number (-)	T	temperature (K)
U	heat transfer coefficient ($W \cdot m^{-2} \cdot K^{-1}$)	V	velocity ($m \cdot s^{-1}$)
V_s	swept volume ($m^3 \cdot s^{-1}$)	$\dot{W}$	mechanical work (W)

REFERENCES

Adamson B.M., 2008. Application of hydrocarbon refrigerants with scroll compressors in low temperature cascade systems. In: Proceedings of the IIR Gustav Lorentzen Conference on Natural Refrigerants, Copenhagen, Denmark, IIF/IIR, 126-130.

Blunier B., Cirrincione G., Herve Y., Miraouia A., 2009. A new analytical and dynamical model of a scroll compressor with experimental validation. Int. J. Refrigeration 32, 874-891.

Byrne P, Miriel J, Lénat Y., 2008. Design and simulation of a heat pump for simultaneous heating and cooling using HFC or CO_2 as a working fluid. In: Proceedings of the IIR Gustav Lorentzen Conference on Natural Refrigerants, Copenhagen, Denmark, IIF/IIR, .484-491.

Byrne P, Miriel J, Lénat Y., 2009. Design and simulation of a heat pump for simultaneous heating and cooling using HFC or CO_2 as a working fluid. Int. J. Refrigeration 32, 1711-1723.

Byrne P, Miriel J, Lénat Y., 2011a. Experimental study of an air-source heat pump for simultaneous heating and cooling – part 1: basic concepts and performance verification. Applied Energy 88, 1841-1847.

Byrne P, Miriel J, Lénat Y., 2011b. Experimental study of an air-source heat pump for simultaneous heating and cooling – part 2: dynamic behaviour and two-phase thermosiphon defrosting technique. Applied Energy 88, 3072-3078

Chen Y., Halm N.P., Groll E.A., Braun J.E., 2002a. Mathematical modeling of scroll compressors - part I: compression process modelling. Int. J. Refrigeration 25, 731-750.

Chen Y., Halm N.P., Braun J.E., Groll E.A., 2002b. Mathematical modeling of scroll compressors - part II: overall scroll compressor modeling. Int. J. Refrigeration 25, 751-764.

Cuevas C., Lebrun J., 2009. Testing and modelling of a variable speed scroll compressor. Applied Thermal Engineering 29, 469-478.

Cuevas C., Lebrun J., Lemort V., Winandy E., 2010. Characterization of a scroll compressor under extended operating conditions. Applied Thermal Engineering 30, 605–615.

Duprez M.-E., Dumont E., Frère M. 2007. Modelling of reciprocating and scroll compressors. Int. J. Refrigeration 30, 873-886.

Duprez M.-E., Dumont E., Frère M. 2010. Modeling of scroll compressors – Improvements. Int. J. Refrigeration 33, 721-728.

Klein S.A., Alvarado F.L., 2000. EES – Engineering Equation Solver, F-Chart software, Wisconsin, USA.

Kinab E., Marchio D., Rivière P., Zoughaib A., 2010. Reversible heat pump model for seasonal performance optimization. Energy and Buildings 42, 2269-2280.

Sun S., Zhao Y., Li L., Shu P., 2010. Simulation research on scroll refrigeration compressor with external cooling. Int. J. Refrigeration 33, 897-906.

Tseng C.-H., Chang Y.-C., 2006. Family design of scroll compressors with optimization. Applied Thermal Engineering 26, 1074-1086.

Winandy E., Saavedra C., Lebrun J., 2002a. Experimental analysis and simplified modelling of a hermetic scroll refrigeration compressor. Applied Thermal Engineering 22, 107-120.

Winandy E., Lebrun J., 2002b. Scroll compressors using gas and liquid injection: experimental analysis and modelling. Int. J. Refrigeration 25, 1143-1156.